Notes

Stereochemical Influences on Intervalence Charge Transfer in Homodinuclear Complexes of Ruthenium

Deanna M. D′Alessandro, Laurence S. Kelso, and F. Richard Keene*

School of Pharmacy & Molecular Sciences,
James Cook University, Townsville,
Queensland 4811, Australia

Received September 24, 2001

Introduction

The synthesis of polynuclear transition metal assemblies and their electrochemical, photochemical, and photophysical properties have attracted significant recent interest; this has been motivated largely by the potential of multicomponent systems as a basis of novel applicable materials.[1] However, the existence of the stereochemical complexities inherent in such systems, and their influence on intramolecular energy- and electron-transfer processes, has not always been acknowledged.[2]

Work in our laboratory has established synthetic methodologies for the isolation of the stereoisomers of a variety of mono-, di-, and trinuclear complexes.[2,3] Significantly, this work has given rise to the first three examples of differences in the spectral, electrochemical, and photophysical properties of stereoisomers in such assemblies.[2,4]

We now report the first investigation of the influence of stereochemical factors on intervalence charge transfer (IT). Importantly, this work has revealed a dependence of the IT characteristics (including thermochromism) and redox properties on stereochemical identity in two dinuclear complexes.

Results and Discussion.

The systems studied were of the type $[\{Ru(bpy)_2\}_2(\mu\text{-BL})]^{4+}$, where BL represents the structurally-related ligands 2,3-bis(2-pyridyl)-1,4-benzoquinoxaline (dpb) and dipyrido(2,3-a;3′,2′-c)benzophenazine (dpb′) (shown in Figure 1). The dinuclear species each exist in two diastereoisomeric forms, meso ($\Delta\Lambda$) and rac, the latter comprising an enantiomeric pair ($\Delta\Delta$ and $\Lambda\Lambda$).[3] Both bridging ligands possess unoccupied low-lying π^* orbitals and mediate electronic coupling between the metal centers via the superexchange-assisted electron-transfer mechanism.[5]

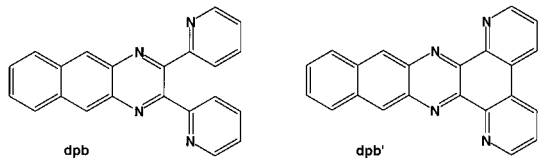

Figure 1. The dpb and dpb′ bridging ligands.

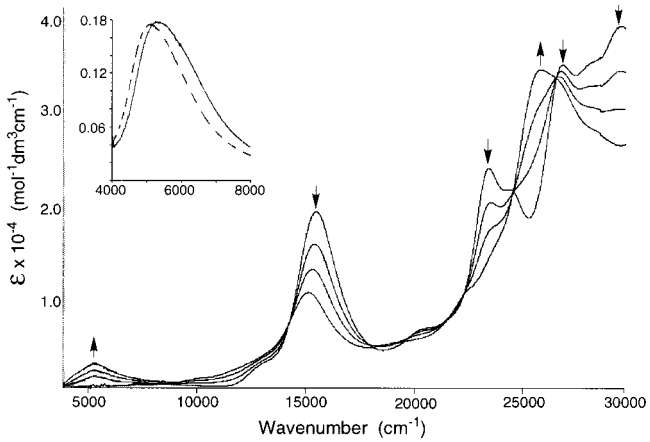

Figure 2. Spectroelectrochemical changes for the oxidation reaction *meso*-$[Ru^{II}(bpy)_2(\mu\text{-dpb})Ru^{II}(bpy)_2]^{4+} \rightarrow$ *meso*-$[Ru^{III}(bpy)_2(\mu\text{-dpb})Ru^{II}(bpy)_2]^{5+}$ at −35 °C.[6] Inset shows IT bands for *meso*-$[Ru^{III}(bpy)_2(\mu\text{-dpb})Ru^{II}(bpy)_2]^{5+}$ (—) and *rac*-$[Ru^{III}(bpy)_2(\mu\text{-dpb})Ru^{II}(bpy)_2]^{5+}$ (− − −).

Electrochemically, cyclic voltammetry studies of each species revealed two reversible one-electron redox processes corresponding to successive oxidation of the metal centers, and multiple reversible ligand-based reductions.[6] The differences between the potentials of the oxidation processes, measured by differential pulse voltammetry ($\Delta E_{ox} = 192 \pm 10$ and 176 ± 10 mV for *meso*- and *rac*-$[\{Ru(bpy)_2\}_2(\mu\text{-dpb})]^{4+}$, respectively; $\Delta E_{ox} = 230 \pm 10$ mV for both *meso*- and *rac*-$[\{Ru(bpy)_2\}_2(\mu\text{-dpb′})]^{4+}$), were sufficient to allow generation of the mixed-valence species in each case.

Spectroelectrochemical studies[6] on the diastereoisomers of $[\{Ru(bpy)_2\}_2(\mu\text{-dpb})]^{4+}$ and $[\{Ru(bpy)_2\}_2(\mu\text{-dpb′})]^{4+}$ at −35 °C revealed stable isosbestic points for the first oxidation process, producing $[(bpy)_2Ru^{III}(\mu\text{-BL})Ru^{II}(bpy)_2]^{5+}$, accompanied by a decrease in the intensity of their respective MLCT absorptions (in the range 13900−17900 cm^{-1}). The $d\pi(Ru)^{II} \rightarrow p^*$(BL) band collapsed completely on removal of the second electron. The first oxidation for the complexes was also characterized by the appearance of a new band in the region 5110−5340 cm^{-1}, which collapsed completely on further oxidation to the +6 species: on this basis, the band was assigned as an IT transition. The spectral progression accompanying the formation of the mixed-valence species for the *meso*-$[\{Ru(bpy)_2\}_2(\mu\text{-dpb})]^{4+}$ diastereoisomer is presented in Figure 2. The IT characteristics for the diastereoisomers of both complexes are presented in Table 1.

* To whom correspondence should be addressed.

(1) Balzani, V.; Scandola, F. *Supramolecular Photochemistry*; Ellis Horwood: Chichester (U.K.), 1991; Sauvage, J.-P. *Acc. Chem. Res.* **1998**, *31*, 611.
(2) Keene, F. R. *Coord. Chem. Rev.* **1997**, *166*, 122.
(3) Keene, F. R. *Chem. Soc. Rev.* **1998**, *27*, 185.
(4) Kelso, L. S.; Reitsma, D. A.; Keene, F. R. *Inorg. Chem.* **1996**, *35*, 5144; Rutherford, T. J.; Van Gijte, O.; Kirsch − De Mesmaeker, A.; Keene, F. R. *Inorg. Chem.* **1997**, *36*, 4465; Rutherford, T. J.; Keene, F. R. *Inorg. Chem.* **1997**, *36*, 2872; Treadway, J. A.; Chen, P.; Rutherford, T. J.; Keene, F. R.; Meyer, T. J. *J. Phys. Chem. A* **1997**, *101*, 6824.
(5) Giuffrida, G.; Campagna, S. *Coord. Chem. Rev.* **1994**, *135*, 517.

(6) Acetonitrile/0.1 mol dm^{-3} $[(n\text{-}C_4H_9)_4N]PF_6$ solution versus Ag/AgCl; Pt or glassy carbon working electrode.

10.1021/ic010857c CCC: $20.00
Published on Web 11/17/2001

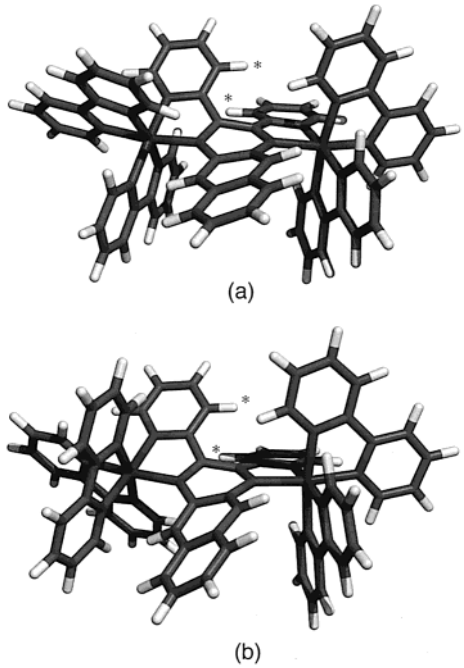

Figure 3. PM3(tm) geometry optimized structures[7] of the diastereoisomeric ΔΛ (a) and ΔΔ (b) forms of $[\{Ru(bpy)_2\}_2(\mu\text{-dpb})]^{4+}$. The H(3) protons on the two pyridyl rings are indicated by asterisks.

Table 1. Properties of the Intervalence Transition of the Mixed-Valence Complexes $[\{Ru(bpy)_2\}_2(\mu\text{-Bl})]^{5+}$ {BL = dpb, dpb′} at −35 °C[6]

complex	E_{op} (±10) (cm^{-1})	ϵ_{max} (±10) ($mol^{-1}dm^3\ cm^{-1}$)	$\Delta\nu_{1/2}$ (±20) (cm^{-1})
meso-$[\{Ru(bpy)_2\}2(\mu\text{-dpb})]^{5+}$	5340	1790	2250
rac-$[\{Ru(bpy)_2\}_2(\mu\text{-dpb})]^{5+}$	5110	1750	2020
meso-$[\{Ru(bpy)_2\}_2(\mu\text{-dpb}')]^{5+}$	5300	4610	1130
rac-$[\{Ru(bpy)_2\}_2(\mu\text{-dpb}')]^{5+}$	5320	3580	1230

There are measurable differences in the characteristics of the IT bands between not only the different complexes, but also between the diastereoisomers of the same complex. For both complexes, the intensities of the IT bands (ϵ_{max}) for the meso diastereoisomers were higher than those for the corresponding rac forms, suggesting a greater degree of metal−metal interaction in the former. The difference of 230 ± 20 cm^{-1} observed between the energies of the IT band maxima (E_{op}) for the diastereoisomers of $[\{Ru(bpy)_2\}_2(\mu\text{-dpb})]^{5+}$ lies well outside the limits of experimental error.

The equilibrium geometries of the diastereoisomers were examined using semiempirical PM3(tm) techniques[7] to provide an insight into differential structural features induced by the stereochemistry. These gas-phase calculations predicted significant distortions in the conformations of the bridging ligands; in particular, the PM3(tm) minimized forms of $[\{Ru(bpy)_2\}_2(\mu\text{-dpb})]^{4+}$ (Figure 3) revealed considerable distortion of the central pyrazine rings, a twist in the benzoquinoxaline "tail" of the bridges, and a large dihedral skew of the two pyridyl rings of the bridge arising from steric interaction of the H(3) protons. Interestingly, the dihedral angle subtended by the pyridyl rings was greater in the rac form (38.4 versus 36.8°), as was the degree of twist in the benzoquinoxaline "tail" compared with that of the meso structure.[8] In contrast, for the analogous system containing the dpb′ ligand, the C−C bond connecting the C(3) atoms prevents the lateral movement of the pyridyl rings in both diastereoisomers (Figure 4).

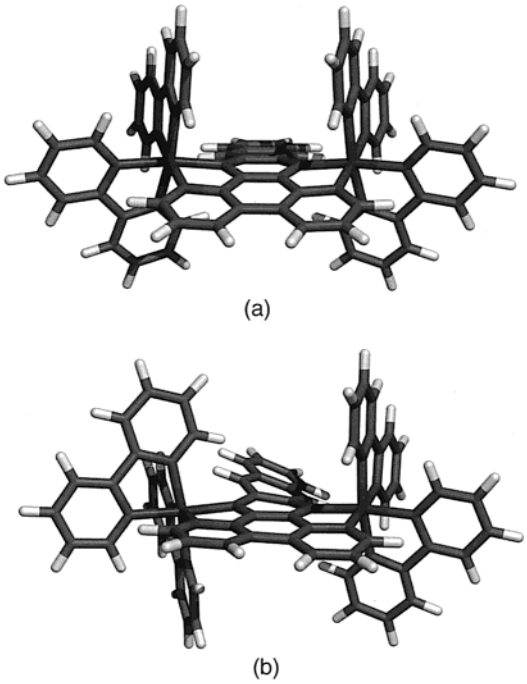

Figure 4. PM3(tm) geometry optimized structures[7] of the diastereoisomeric ΔΛ (a) and ΔΔ (b) forms of $[\{Ru(bpy)_2\}_2(\mu\text{-dpb}')]^{4+}$.

The significant structural differences between the diastereoisomeric forms of the two complexes prompted an examination of the distribution of the ligand-based frontier orbitals which mediate electron-transfer between the metal centers.[7] Of particular interest was whether these structural differences would translate into measurable differences in the electronic characteristics of the diastereoisomers. In the meso form of $[\{Ru(bpy)_2\}_2(\mu\text{-dpb})]^{4+}$, the LUMOs were distributed across the entire surface of the bridge with the highest densities on the pyrazine ring and the adjacent phenyl ring. In comparison, the LUMOs of the rac form were more localized, being located solely on the benzoquinoxaline region of the bridge. For $[\{Ru(bpy)_2\}_2(\mu\text{-dpb}')]^{4+}$, no significant differences were found between the diastereoisomers; the LUMO was distributed across the entire bridge, with the highest densities on the pyrazine and the two adjacent phenyl rings.

The differing spectral and electrochemical characteristics of the diastereoisomers appear to be consistent with the variations observed in the structural features and molecular orbital distributions, which are a consequence of the different stereochemistries of the species. For example, the ΔE_{ox} values for the diastereoisomers of $[\{Ru(bpy)_2\}_2(\mu\text{-dpb}')]^{4+}$ are greater than those of $[\{Ru(bpy)_2\}_2(\mu\text{-dpb})]^{4+}$, since the degree of metal−metal communication is greater for those structures where the bridging ligand assumes a less distorted conformation. Moreover, the greater ΔE_{ox} for the meso form of $[\{Ru(bpy)_2\}_2(\mu\text{-dpb})]^{4+}$, relative to the corresponding rac form, may reflect the relatively greater degree of structural distortion evident in the molecular model of the latter.

An investigation of the thermochromic behavior of the IT transitions in butyronitrile/0.1 mol dm^{-3} $[(n\text{-}C_4H_9)_4N]PF_6$ solu-

(7) *SPARTAN*, Version 5.0; Wavefunction Inc.: Irvine, CA, 1997.

(8) The nature of the structural distortions obtained in the geometry optimizations are closely reflected in X-ray crystal structures of the *meso*-$[\{Ru(bpy)_2\}_2(\mu\text{-dpb})]^{4+}$ cation. (D′Alessandro, D. M.; Junk P. C.; Keene, F. R., unpublished results).

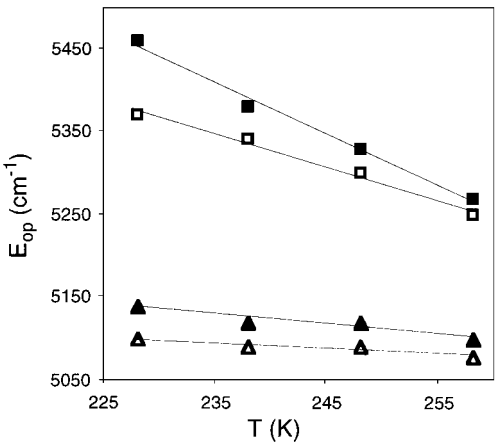

Figure 5. E_{op} as a function of temperature for the diastereomeric forms of $[\{Ru(bpy)_2\}_2(\mu\text{-dpb})]^{5+}$: meso (■) and rac (▲) in butyronitrile/0.1 mol dm^{-3} $[(n\text{-}C_4H_9)_4N]PF_6$ solution; meso (□) and rac (Δ) in butyronitrile/0.02 mol dm^{-3} $[(n\text{-}C_4H_9)_4N]\{B(C_6F_5)_4\}$ solution.

tion revealed different temperature responses for the two complexes and variations between the diastereoisomeric forms of the same species. Over the temperature range examined, the energies of the IT band maxima were independent of temperature for the diastereoisomers of $[\{Ru(bpy)_2\}_2(\mu\text{-dpb}')]^{5+}$. However, for the diastereoisomers of $[\{Ru(bpy)_2\}_2(\mu\text{-dpb})]^{5+}$, a red shift in the IT bands was observed with an increase in temperature, the effect being considerably greater for the meso isomer: from the linear variation (Figure 5), $dE_{op}/dT = -6.7 \pm 0.4$ cm^{-1} K^{-1} (meso) and -1.2 ± 0.2 cm^{-1} K^{-1} (rac).

Within the theoretical framework of the Marcus−Hush theory of intervalence charge transfer, the energy of the IT transition is given by $E_{op} = \lambda_{inner} + \lambda_{outer} + \Delta E + \Delta E'$.[9,10] The contributions λ_{inner}, λ_{outer}, and $\Delta E'$ are unlikely to have a significant temperature dependence,[11] so the thermochromism of the IT band arises primarily from the redox asymmetry term ΔE. However, in view of the similar coordination environments of the diastereoisomers of the two complexes, this term should be negligible. In addition to the structural distortions observed in the bridging ligands (Figures 3 & 4), ion-pairing effects,[12] which are more pronounced at lower temperatures, will result in nonzero ΔE values. The latter are known to cause the IT band to broaden and shift toward lower energy with increasing temperature, as observed in the present study.

To assess the influence of ion-pairing effects, the thermochromism of the IT transitions for $[\{Ru(bpy)_2\}_2(\mu\text{-dpb})]^{5+}$ was investigated in butyronitrile/0.02 mol dm^{-3} $[(n\text{-}C_4H_9)_4N]\{B(C_6F_5)_4\}$ solution, since the $\{B(C_6F_5)_4\}^-$ anion is known to associate weakly in comparison with PF_6^-.[13] As with the PF_6^- electrolyte, the IT bands were red-shifted with an increase in temperature, however, the effect was significantly less pronounced in the presence of the $\{B(C_6F_5)_4\}^-$ anion: from the linear variation $dE_{op}/dT = -4.0 \pm 0.3$ cm^{-1} K^{-1} (meso) and -0.6 ± 0.1 cm^{-1} K^{-1} (rac). This suggests that ion pairing has a significant effect on the redox asymmetry and, hence, the thermochromic behavior of the IT transitions in the species investigated. Importantly, the greater temperature dependence of *meso*-$[\{Ru(bpy)_2\}_2(\mu\text{-dpb})]^{5+}$ relative to the corresponding rac form appears to reflect the greater extent of ion pairing in the former. Indeed, the preferential interaction of the meso isomer with anions accounts for the increased rate of elution of this isomer in the cation exchange separation process.[14]

The present study has detailed the first observation of the influence of stereochemistry on intervalence charge transfer. The elucidation of the factors involved will be significant in completing our understanding of intramolecular energy- and electron-transfer processes.

Experimental Section

Materials. $[Ru(bpy)_2Cl_2]\cdot 2H_2O$,[15] 4,7-phenanthroline-5,6-dione,[16] $[(n\text{-}C_4H_9)_4N]\{B(C_6F_5)_4\}$,[13] and 2,3-bis(2-pyridyl)-1,4-benzoquinoxaline (dpb)[17] were prepared according to literature procedures. Butyronitrile (99+ %, Aldrich), $[(n\text{-}C_4H_9)_4N]PF_6$ (Fluka), 2,3-diaminonaphthalene (Fluka), and sodium toluene-4-sulfonate (Aldrich) were used as received. Acetonitrile was distilled under nitrogen from CaH_2 immediately prior to use.

Physical Methods. ^1H NMR and COSY experiments were performed on a Varian Mercury 300 MHz NMR spectrometer at room temperature using CD_3CN and $CDCl_3$ as solvents. Elemental analyses were performed within the Department of Chemistry at James Cook University.

Electrochemical measurements were performed under argon using a Bioanalytical Systems BAS 100A electrochemical analyzer. Cyclic and differential pulse voltammograms were recorded in acetonitrile/0.1 mol dm^{-3} $[(n\text{-}C_4H_9)_4N]PF_6$ solution using a glassy carbon or platinum button working electrode, a platinum wire auxiliary electrode, and a Ag/AgCl (0.1 mol dm^{-3} $[(n\text{-}C_4H_9)_4N]PF_6$ in acetonitrile) reference electrode. Ferrocene was added as an internal standard upon completion of each experiment (the ferrocene/ferrocenium couple occurred at +550 mV versus Ag/AgCl). Cyclic voltammetry was performed with a sweep rate of 100 mV s^{-1}; differential pulse voltammetry was conducted with a sweep rate of 4 mV s^{-1} and a pulse amplitude, width, and period of 50 mV, 60 ms, and 1 s, respectively.

The electronic absorption spectra of the electrogenerated mixed-valence species were recorded in situ using a cryostatic optically semi-transparent thin-layer electrochemical (OSTLE) cell in the path of a CARY 5E UV/vis/NIR spectrophotometer. Appropriate potentials were applied using a BAS CV27 voltammograph. The reversibility of the spectral data was checked by the regeneration of the starting material; the observation of stable isosbestic points and regeneration of the starting spectrum were indicative of the chemical reversibility of all redox processes.

Computational Methods. The 3D structures of the diastereoisomers were composed using the CS Chem3D program,[18] and the resultant structures were optimized using the semiempirical PM3(tm) method implemented in the SPARTAN program[7] on an SGI Power Challenge XL. The HOMO and LUMO distributions of the optimized structures were subsequently determined. All parameters employed were at their default values, with the converge command invoked to assist convergence in the SCF procedure after a maximum of 1000 geometry optimization cycles.

Dipyrido(2,3-a;3′2′-c)benzophenazine (dpb′). A methanolic solution (20 cm^3) of 2,3-diaminonaphthalene (0.42 g, 2.5 mmol) and 4,7-

(9) Creutz, C. *Prog. Inorg. Chem.* **1983**, *30*, 1; Crutchley, R. J. *Adv. Inorg. Chem.* **1994**, *41*, 273.
(10) ΔE is the thermodynamic energy difference between the equilibrium vibrational states of the two different redox isomers; λ_{inner} and λ_{outer} are the reorganizational energies for the inner and outer nuclear modes, respectively; $\Delta E'$ is an additional term reflecting possible energy contributions due to spin−orbit coupling effects and/or ligand field asymmetry.
(11) Dong, Y.; Hupp, J. T. *Inorg. Chem.* **1992**, *11*, 3323.
(12) Lewis, N. A.; Obeng, Y. S.; Purcell, W. L. *Inorg. Chem.* **1989**, *28*, 3796; Lewis, N. A.; Obeng, Y. S. *J. Am. Chem. Soc.* **1988**, *110*, 2306; Blackbourn, R. L.; Hupp, J. T. *Chem. Phys. Lett.* **1998**, *150*, 399; Johnson, R. C.; Hupp, J. T. *J. Am. Chem. Soc.* **2001**, *123*, 2053.
(13) LeSuer, R. J.; Geiger, W. E. *Angew. Chem., Int. Ed.* **2000**, *39*, 248.
(14) Fletcher, N. C.; Keene, F. R. *J. Chem. Soc., Dalton Trans.* **1999**, 683.
(15) Togano, T.; Nagao, N.; Tsuchida, M.; Kumakura, H.; Hisamatsu, K.; Scott Howell, F.; Mukaida, M. *Inorg. Chim Acta* **1992**, *195*, 221−225.
(16) Druey, J.; Schmidt, P. *Helv. Chim. Acta* **1950**, *33*, 1080−1087.
(17) Yeomans, B. D.; Kelso, L. S.; Tregloan, P. A.; Keene, F. R. *Eur J. Inorg. Chem.* **2001**, 239.
(18) *CS Chem3D Pro*, Version 4.0; CambridgeSoft Corporation: Cambridge, MA, 1997.

phenanthroline-5,6-dione (0.5 g, 2.4 mmol) was refluxed for 0.5 h. Water was added, and the volume was reduced via rotary evaporation. The yellow crystalline solid was collected by filtration and recrystallized from methanol. Yield: 0.662 g (83%). ^{1}H NMR ($CDCl_3$): δ (ppm) 7.64 (2H, dd), 7.81 (2H, dd), 8.24 (2H, dd), 8.86 (2H, d), 9.29 (2H, d), 9.30 (2H, s). Anal. Calcd for $C_{22}H_{12}N_4$: C, 79.5; H, 3.64; N, 16.9. Found: C, 79.9; H, 3.96; N, 16.4.

[{Ru(bpy)$_2$}$_2$(μ-dpb)](PF$_6$)$_4$: was prepared according to the literature procedure.[17] Diastereoisomeric ratio (meso/rac) = 56:44. The identity of the meso diastereomer was confirmed from X-ray crystal structures of the [{Ru(bpy)$_2$}$_2$(μ-dpb)]$^{4+}$ cation.[8] Anal. Calcd for $C_{62}H_{46}N_{12}F_{24}P_4Ru_2$: C, 42.8; H, 2.66; N, 9.6. Found: (meso) C, 42.6; H, 2.74; N, 9.5; (rac) C, 42.8; H, 2.58; N, 9.3. ^{1}H NMR (CD_3CN): δ (ppm) (meso*)* 6.58 (2H, J = 5, 1.5 Hz, dd), 6.97 (2H, J = 5, 1.5 Hz, dd), 7.18 (2H, J = 8, 5 Hz, dd), 7.26 (2H, J = 8, 5 Hz, dd), 7.38−7.68 (10H, m), 7.72−8.40 (12H, m), 8.49 (2H, J = 8, 1.5 Hz, dd), 8.58 (2H, J = 8, 1.5 Hz, dd), 8.60 (2H, J = 8, 1.5 Hz, dd), 8.75 (4H, J = 8, 1.5 Hz, dd), 8.80 (2H, J = 8, 1.5 Hz, dd); (rac) 7.09 (2H, J = 8, 5 Hz, dd), 7.34 (2H, dd), 7.45 (4H, J = 8, 5 Hz, dd), 7.53 (2H, dd), 7.62 (2H, J = 8, 5 Hz, dd), 7.64 (2H, J = 5, 1.5 Hz, dd), 7.70 (2H, J = 5, 1.5 Hz, dd), 7.79 (2H, J = 5, 1.5 Hz, dd), 8.00 (2H, J = 8, 8 Hz, dd), 8.06 (2H, J = 8, 8 Hz, dd), 8.06 (2H, s), 8.07−8.10 (6H, m), 8.11 (2H, J = 8, 8 Hz, dd), 8.20 (2H, J = 8, 8 Hz, dd), 8.23 (2H, J = 5, 1.5 Hz, dd), 8.31 (2H, J = 8, 1.5 Hz, dd), 8.33 (2H, J = 8, 1.5 Hz, dd), 8.67 (2H, dd), 8.68 (2H, J = 8, 1.5 Hz, dd), 8.71 (2H, J = 8, 1.5 Hz, dd).

[{Ru(bpy)$_2$}$_2$(μ-dpb′)](PF$_6$)$_4$. This complex was prepared from dpb′ (25 mg; 0.075 mmol) and [Ru(bpy)$_2$Cl$_2$]·2H$_2$O (85 mg, 0.165 mmol) in an analogous manner to the preparation of [{Ru(bpy)$_2$}$_2$(μ-dpb)](PF$_6$)$_4$.[18] Yield: 93 mg (71%). The diastereoisomeric proportions were meso/rac = 63/37. Anal. Calcd for $C_{62}H_{44}N_{12}F_{24}P_4Ru_2$: C, 42.8; H, 2.55; N, 9.7. Found: (meso) C, 42.5; H, 2.58; N, 9.6; (rac) C, 42.8; H, 2.55; N, 9.7. ^{1}H NMR (CD_3CN):δ (ppm) (meso*)* 6.97 (2H, J = 5, 1.5 Hz, dd), 7.15 (2H, J = 8, 5 Hz, dd), 7.25 (1H, J = 8, 5 Hz, dd), 7.33 (2H, dd), 7.48 (2H, J = 8, 5 Hz, dd), 7.58 (2H, dd), 7.70 (2H, J = 8, 5 Hz, dd), 7.72 (2H, J = 5, 1.5 Hz, dd), 7.75 (2H, J = 5, 1.5 Hz, dd), 7.76 (2H, J = 8, 8 Hz, dd), 7.97 (2H, J = 5, 1.5 Hz, dd), 7.98 (2H, dd), 8.06 (2H, J = 8, 1.5 Hz, dd), 8.13 (2H, J = 8, 8 Hz, dd), 8.16 (2H, d), 8.19 (2H, J = 8, 8 Hz, dd), 8.24 (2H, J = 8, 8 Hz, dd), 8.24 (2H, s), 8.27 (2H, J = 8, 1.5 Hz, dd), 8.69 (2H, J = 8, 1.5 Hz, dd), 8.72 (2H, J = 8, 1.5 Hz, dd), 9.33 (2H, d); (rac) 7.01 (2H, J = 8, 5 Hz, dd), 7.15 (2H, dd), 7.25 (2H, J = 8, 5 Hz, dd), 7.34 (2H, J = 5, 1.5 Hz, dd), 7.54 (2H, J = 5, 1.5 Hz, dd), 7.54 (2H, J = 8, 5 Hz, dd), 7.57 (2H, dd), 7.62 (2H, J = 8, 5 Hz, dd), 7.68 (2H, J = 5, 1.5 Hz, dd), 7.99 (2H, dd), 8.00 (2H, J = 5, 1.5 Hz, dd), 8.02 (2H, J = 8, 8 Hz, dd), 8.05 (2H, J = 8, 8 Hz, dd), 8.07 (2H, s), 8.18 (2H, d), 8.21 (2H, J = 8, 8 Hz, dd), 8.25 (2H, J = 8, 8 Hz, dd), 8.45 (2H, J = 8, 1.5 Hz, dd), 8.57 (2H, J = 8, 1.5 Hz, dd), 8.57 (2H, J = 8, 1.5 Hz, dd), 8.63 (2H, J = 8, 1.5 Hz, dd), 9.26 (2H, d).

Acknowledgment. We thank Professor J. T. Hupp for helpful discussions on the manuscript, and we gratefully acknowledge the financial support of the Australian Research Council.

IC010857C